COMPDYN 2013
4th ECCOMAS Thematic Conference on
Computational Methods in Structural Dynamics and Earthquake Engineering
M. Papadrakakis, V. Papadopoulos, V. Plevris (eds.)
Kos Island, Greece, 12–14 June 2013

TOWARDS A UNIFIED DESCRIPTION OF ROCKING STRUCTURES

Matthew J. DeJong[1], **Elias G. Dimitrakopoulos**[2]

[1] University of Cambridge
Department of Engineering, Trumpington Street, Cambridge, CB2 1PZ, United Kingdom
e-mail: mjd97@cam.ac.uk

[2] Hong Kong University of Science and Technology
Department of Civil and Environmental Engineering, Kowloon, Clear Water Bay, Hong Kong
ilias@ust.hk

Keywords: rocking, self-centering, rocking spectra, analytical dynamics, equivalent systems.

Abstract. *Numerous studies on the rigid rocking block have generated a wealth of knowledge about rocking behavior. However, evaluation of more complex rocking systems requires the derivation and solution of complicated equations of motion. This paper investigates the possibility of a unified description of several rocking systems through investigation of rocking mechanisms which describe the masonry wall and the masonry arch. Effective rocking parameters are derived for each of these structures, and the similarity of the rocking behavior is discussed. The error of the proposed approximation, which defines the limitations for this approach, is quantified for the example structures considered. Where appropriate, a unified description of rocking would allow the use of rocking spectra, which would be useful to readily predict the response of a wide array of rocking structures.*

1 INTRODUCTION

The concept of re-centering structures, which use some degree of rocking motion to isolate a structure from the stresses induced by earthquakes, is becoming increasingly investigated as a modern seismic design alternative. Anecdotally, this beneficial isolating effect has been proposed as an explanation for the ability of some monumental masonry structures to survive large earthquake events. Despite these claims, the assessment of existing masonry structures which may be susceptible to rocking overturning collapse during earthquakes remains a difficult task.

This paper describes continued investigations regarding the use of rocking spectra, derived by considering the response of a single rigid rocking block, to predict the maximum response of a much wider range of structures. In order for this to be possible, equivalent rocking blocks must be defined for a range of more complex rocking mechanisms.

In this paper, rocking structures which have already been demonstrated to exhibit direct equivalence with a single rigid block are first reviewed. For these structures, the use of rocking spectra to predict response is more obvious. Subsequently, two rocking mechanisms will be considered which exhibit more complex kinematics. Equivalence between these structures and a single rigid block is sought. In this context, the error associated with required simplifying assumptions is quantified. In the process, the equations of motion are presented in general form in order to provide a more unified description of complicated rocking structures.

2 REVIEW OF SIMPLE ROCKING STRUCTURES

This section briefly reviews the equations of motion governing the response of the single rigid rocking block and discusses other rocking structures which are dynamically equivalent.

2.1 The rocking block

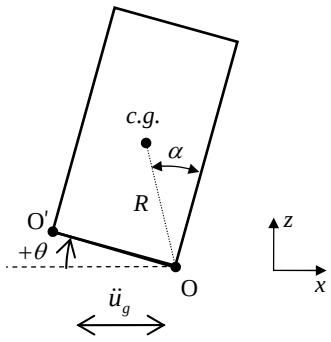

Figure 1: Geometry of the rocking block.

The equation of motion for positive rotation of the rocking block shown in Fig. 1 can be written [1]:

$$\ddot{\theta} = p^2 \left(-\sin\left(\theta_{cr} - \theta\right) - \frac{\ddot{u}_g}{g} \cos\left(\theta_{cr} - \theta\right) \right) \tag{1}$$

where $p^2 = 3g/4R$, $\theta_{cr} = \alpha$, and $\ddot{u}_g$ is the horizontal acceleration of the ground. According to Eqn. (1), the ground motion ($\ddot{u}_g / g$) required to initiate rocking motion is $\lambda = \tan\alpha$. When

the block returns to its initial position, impact occurs causing a dissipation of energy which can be approximated by a coefficient of restitution:

$$\eta = \dot{\theta}^{+} / \dot{\theta}^{-} \tag{2}$$

where $\dot{\theta}^{-}$ and $\dot{\theta}^{+}$ are the angular velocity before and after impact respectively. Conservation of momentum equations are often used to estimate the coefficient of restitution [1], but it will be left as an independent parameter in this paper. An equation similar to (1) can then be used for negative rotations ($\theta_{cr} = -\alpha$) about the point O′ in Fig. 1 [1].

While Eqn. (1) can be solved numerically, it is convenient to linearize it about the point of unstable equilibrium (θ_{cr}), yielding:

$$\ddot{\theta} = p^2 \left(\theta_{cr} - \theta - \frac{\ddot{u}_g}{g} \right) \tag{3}$$

According to Eqn. (3), the ground acceleration ($\ddot{u}_g / g$) required to initiate rocking motion of the linearized system is $\lambda_{lin} = \alpha$.

The error in predicting the rocking response using Eqn. (3) as opposed to Eqn. (1) increases as the slenderness decreases. Generally, the assumed analytical model is only reasonable for relatively slender blocks where sliding and bouncing can be neglected. For these same slender geometries, the errors associated with linearization are small when compared to the uncertainty involved in predicting expected ground motions, so Eqn. (3) is practically useful.

2.2 Equivalent rocking structures

The analytical model presented in §2.1 has been extensively used to study the response of the rigid rocking block to a wide variety of ground motions (e.g. harmonic [2], pulses [3], real earthquake time histories [4], synthetic earthquake time histories [1,5]). These studies have yielded a wealth of knowledge regarding the behavior of rocking structures. However, application of this knowledge to more complicated structures has been relatively limited.

Clearly, any single rigid body which rocks about alternating corners can be described by Eqns. (1) or (3) by deriving appropriate expressions for p, θ_{cr} and λ. Derivation of these parameters is trivial for some structures, but tedious for others. Regardless, if these parameters can be derived, then rocking response spectra, which predict the maximum response of a single rocking block to a given ground motion, could be used to predict the maximum response. For example, rocking spectra for pulse ground motions (e.g. [6]) are generally applicable to all single rigid bodies.

While the use of rocking spectra for single block structures may seem trivial, these spectra are particularly useful for masonry structures composed of multiple blocks where numerous displacement mechanisms could form. For example, when considering the rocking collapse of masonry spires [7], numerous possible collapse mechanisms were rapidly considered using pulse-based rocking spectra, in order to predict the mechanism which is dynamically most vulnerable to overturning collapse. It should be noted that the governing mechanism is dependent on the pulse characteristics, and is generally different than the mechanism predicted using static methods [7]. Further, single block rocking spectra results compared well with results from detailed computational and experimental models involving numerous blocks [8].

The application of rocking spectra to multiple block rocking mechanisms is the primary focus of this paper. The symmetric three-block frame considered by Makris and Vassiliou [9]

provides a unique example of a multiple block mechanism which has direct equivalence with the rocking block. More general rocking mechanisms are considered in the following section.

3 ROCKING MECHANISMS

In general, the large displacement response of multiple-member kinematic mechanisms is highly nonlinear, and differs between configurations. However, for many structures, the rotation required to reach a point of unstable equilibrium (θ_{cr}), and therefore possible overturning, is relatively small. Thus, the aim of this section is to investigate an approximate equivalence between multiple-member mechanisms and the single rocking block.

3.1 The masonry wall

An example of mechanism that may rock during earthquake excitation is shown in Fig. 2. Several researchers (e.g. [10,11]) have studied the out of plane behavior of masonry walls using a similar model. A static analysis of the wall yields a relatively small lateral resistance to seismic loading because walls are generally slender. While this static analysis may be appropriate for design, it may be overly conservative for assessment. Instead, a simple procedure which accounts for the 'reserve capacity' resulting from the dynamics of the system [10] is desired.

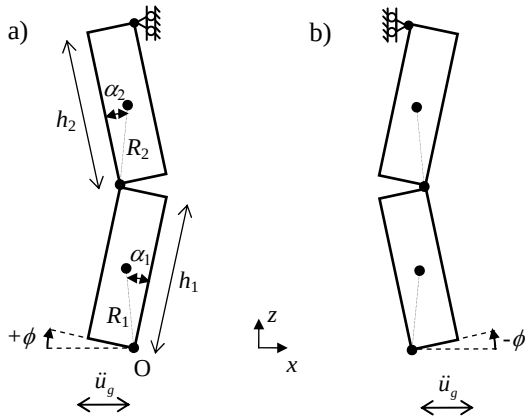

Figure 2: Geometry of the rocking masonry wall for (a) positive and (b) negative rotations.

Wall with mid-height hinge

Initially, it is assumed that a hinge forms at the mid-height of the wall ($\alpha_1 = \alpha_2 = \alpha$, $R_1 = R_2 = R$). The equation of motion of the resulting three-hinge mechanism shown in Fig. 2(a) is:

$$\left(\frac{I_O}{2mR} + 6R\sin^2(\alpha-\phi)\right)\ddot{\phi} - 3R\sin 2(\alpha-\phi)\dot{\phi}^2 + \sin(\alpha-\phi)g = -\frac{1}{2}\ddot{u}_g\cos(\alpha-\phi) \qquad (4)$$

where I_O is the moment of inertia of the bottom block about point O, m is the mass of a single block, and ϕ is the rocking rotation, for which the positive direction is shown in Fig. 2(a). A similar equation could be written for the negative rotation shown in Fig. 2(b). More generally, Eqn. (4) can be written as:

$$I_{nl}(\phi)\ddot{\phi} + J_{nl}(\phi)\dot{\phi}^2 - G_{nl}(\phi)g = -B_{nl}(\phi)\ddot{u}_g \qquad (5)$$

where:

$$\begin{aligned} I_{nl} &= \frac{I_O}{2mR} + 6R\sin^2\left(\alpha - \phi\right) \\ J_{nl} &= 3R\sin 2\left(\alpha - \phi\right) \\ G_{nl} &= \sin\left(\alpha - \phi\right) \\ B_{nl} &= 0.5\cos\left(\alpha - \phi\right) \end{aligned} \tag{6}$$

Note that the ground acceleration ($\ddot{u}_g / g$) which causes initiation of rocking is:

$$\lambda = \left.\frac{G_{nl}}{B_{nl}}\right|_{\phi=0} \tag{7}$$

For the rocking wall in question, $\lambda = 2\tan\alpha$, which is twice the value of free standing block with equal dimensions as one of two blocks composing the wall.

Equation (5) could be solved directly to find the response of the wall to dynamic loading. However, the objective here is to define an equivalent block which can be used to predict the response of the more complicated wall mechanism. Clearly Eqn. (5) is different than Eqn. (1) due to the mechanism kinematics which involve centripetal and Coriolis accelerations. Thus, it is useful to linearize the equation of motion to allow comparison with the rocking block. Linearization of Eqn. (4) about the point of unstable equilibrium ($\phi = \phi_{cr} = \alpha$) yields:

$$\frac{2R}{3}\ddot{\phi} + \left(\phi - \phi_{cr}\right) g = -\frac{1}{2}\ddot{u}_g \tag{8}$$

More generally, Eqn. (8) can be written as:

$$I_{eq}\ddot{\phi} + G_{eq}\left(\phi - \phi_{cr}\right) g = -B_{eq}\ddot{u}_g \tag{9}$$

where $I_{eq} = 2R/3$, $G_{eq} = 1$, and $B_{eq} = 0.5$ for the wall under consideration. Rearranging Eqn. (9) yields:

$$\ddot{\phi} = p_{eq}^2\left(\phi - \phi_{cr} - a_{sc}\frac{\ddot{u}_g}{g}\right) \tag{10}$$

where:

$$p_{eq} = \sqrt{\frac{gG_{eq}}{I_{eq}}} \quad ; \quad a_{sc} = \frac{B_{eq}}{G_{eq}} \tag{11}$$

which yields $p_{eq} = \sqrt{3g/2R} = \sqrt{2}\,p_{block}$ and $a_{sc} = 0.5$ for the wall under consideration. The ground acceleration ($\ddot{u}_g / g$) required to initiate rocking of the linearized system is:

$$\lambda_{lin} = \frac{G_{eq}}{B_{eq}}\phi_{cr} \tag{12}$$

which yields $\lambda_{lin} = 2\alpha$ for the wall under consideration. If the difference between λ and λ_{lin} is small, then the definition of a_{sc} above may be sufficient. However, if the difference is large, then an alternate definition of a_{sc} which preserves the actual uplift acceleration of the nonlinear system may be useful:

$$a_{sc,alt} = \frac{\phi_{cr}}{\lambda} \tag{13}$$

In general, Equation (10) is now similar to Eqn. (3) apart from the a_{sc} term. Thus, the response of a single block can be used to predict the response of the wall mechanism, provided that the acceleration input is scaled by a_{sc}.

While the simplification of the wall to an equivalent block is advantageous, the accuracy of the linear approximation must be evaluated. It is useful to first consider the accuracy under free vibration, where a_{sc} has no effect, and the accuracy is primarily dependent on the estimation of p_{eq}, which results in an effective natural rocking period. It is well documented [1] that the natural rocking period varies with the amplitude of the rocking motion. Thus, the error in the natural rocking period predicted by the equivalent block versus the actual wall ($T_{n,blockeq}$ / $T_{n,wall}$) is plotted in Fig. 3(a) as a function of rocking amplitude (ϕ/ϕ_{cr}). For slender blocks, the error is small, while for stockier blocks the error increases, as expected. In addition, the error is greater for smaller angles of rocking, which results from the linearization about the unstable point of equilibrium ($\phi/\phi_{cr} = 1$). Subsequently, the error associated with a_{sc}, which is directly related to the difference between λ and λ_{lin}, was also considered. The error in the uplift acceleration (λ_{lin}/λ) is plotted in Fig. 3(b), and is generally small.

Finally, the error due to forced vibration was evaluated by considering the time required (t_{over}) for the block to reach the unstable equilibrium position under a constant ground acceleration. The ratio of the overturning time for the linearized system compared to the nonlinear system ($t_{over,blockeq} / t_{over,wall}$) is plotted in Fig. 4, for the values of a_{sc} defined in Eqns. (11) and (13). Again, for slender blocks, the error is relatively small. Further, the effect of using a_{sc} versus $a_{sc,alt}$ is small, and is proportional to the error in uplift acceleration shown in Fig. 3(b), as expected. Thus, either definition of a_{sc} is sufficient for the wall under investigation.

Generally, Figs. 3 and 4 quantify the error associated with the linearization, providing a measure of the confidence with which an equivalent block could be used describe the rocking of a symmetric wall mechanism of a given slenderness.

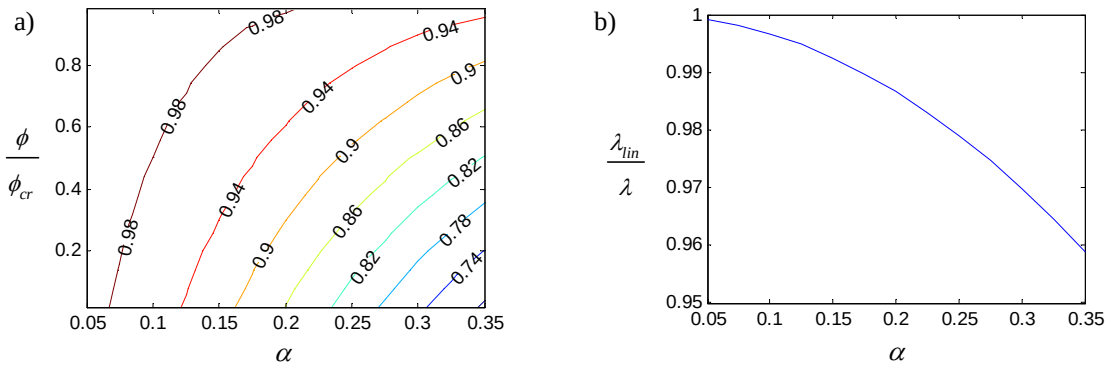

Figure 3: Linearization errors for the masonry wall: (a) natural frequency $T_{n,blockeq}$ / $T_{n,wall}$, (b) uplift acceleration λ_{lin}/λ.

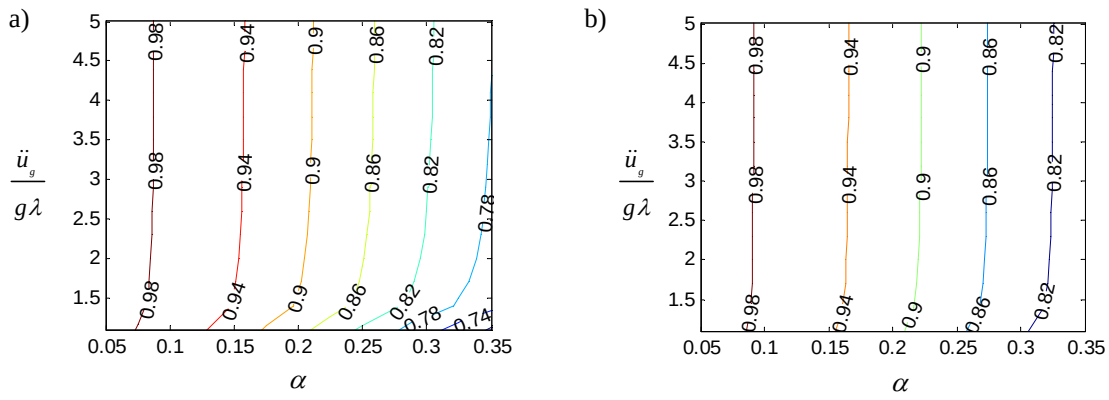

Figure 4: Linearization errors for overturning time ($t_{over,blockeq} / t_{over,wall}$) of the masonry wall due to a constant acceleration of amplitude of $\ddot{u}_g / g\lambda$: (a) a_{sc} , (b) $a_{sc,alt}$.

Wall with arbitrary hinge

If the hinge is not assumed to form at the mid-height of the wall, the equation of motion can still be described by Eqn. (5), but it becomes considerably more complicated than Eqn. (4). Regardless, linearization of the equation of motion about the unstable point of equilibrium ($\phi = \phi_{cr} = \alpha_1$) still yields Eqn. (10), and the equivalent block parameters become:

$$p_{eq} = \sqrt{\frac{3g}{4R_1}\frac{1+2\frac{h_2}{h_1}+\frac{h_2}{h_1}\frac{R_1}{R_2}}{1+\frac{h_2}{h_1}\left(\frac{R_2}{R_1}\right)^2}}$$
$$a_{sc} = 0.5 \tag{14}$$
$$\lambda_{lin} = 2\alpha_1$$

Remarkably, a_{sc} is unaffected by the change in position of the central hinge, while p_{eq} and λ_{lin} vary. In general, smaller scale structures, which correspond to larger values of p_{eq}, are more vulnerable to overturning during an earthquake [1]. For Eqn. (14), p_{eq} is maximum for $h_2/h_1 = 0.74$. However, the initiation of rocking decreases with the height of the central hinge, so an unrealistic structure with $h_2/h_1 = 0$ would be least resistant to rocking initiation. The central hinge height which would be most vulnerable to overturning would therefore be dependent on the ground motion input. For pulse type motions, response spectra [6] could then be used to predict the response for each possible location of the central hinge. Using a similar procedure to previous investigations of masonry spires [7], these spectra could then be used to create a governing response envelope based on all possible mechanisms.

3.2 The masonry arch

Numerous previous studies have used the rigid body mechanism shown in Fig. 5 to analytically describe the dynamic response of the free standing masonry arch. In these studies, the initial hinge locations were found by static analysis, and were then assumed to reflect when the arch returns to its initial position. Despite being a single degree of freedom mechanism, the analytical model proved to effectively predict global collapse when compared to both

computational discrete element modeling [12] and experimental [13] results. Regardless, the aim of this study is again to determine if this complicated four-hinge mechanism can be effectively described by an equivalent single rocking block.

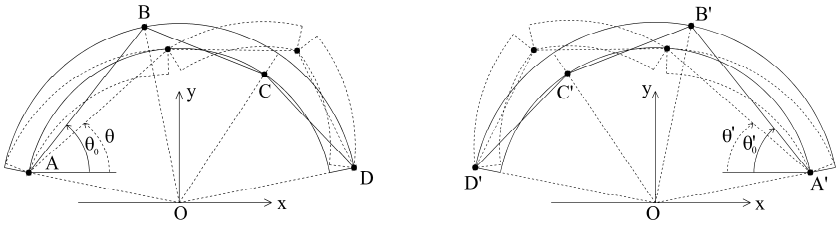

Figure 5: Geometry of the rocking arch.

The equation of motion of the arch in Fig. 5 was derived by Oppenheim [14], and is of the same form as Eqn. (5). The ground acceleration ($\ddot{u}_g / g$) required to uplift the nonlinear system is again described by Eqn. (7). Just as for the two-block rocking wall, the equation of motion can be linearized, resulting in Eqn. (9), and the ground acceleration ($\ddot{u}_g / g$) required for uplift of the linearized system is described by Eqn. (12).

Again it is useful to quantify the error associated with the linearization, which is done using the procedures described in §3.1. For a semi-circular arch (inclusion angle of 180 degrees), the error in natural rocking period ($T_{n,blockeq}$ / $T_{n,arch}$) caused by the linearization is shown in Fig. 6(a) for a range of reasonable thickness to radius ratios (t_a / r). The error is relatively small, and increases as the arch becomes thicker, or less slender, as expected. For the same range of geometries, the error associated with the acceleration which initiates rocking (λ_{lin} / λ) is shown in Fig. 6(b). The error is nearly zero for extremely thin arches, but increases significantly with arch thickness.

To evaluate forced vibration, the error in overturning time ($t_{over,blockeq}$ / $t_{over,arch}$) is shown in Fig. 7, again for the values of a_{sc} defined in Eqns. (11) and (13). Unlike for the wall, the arch results are significantly affected by the definition of a_{sc} due to the kinematics of the mechanism. The error is larger for a_{sc}, but the prediction of maximum response is conservative. The error is smaller for $a_{sc.alt}$, but the prediction of maximum response is unconservative. As a compromise, an average value of a_{sc} could be taken to provide a conservative prediction with reduced error.

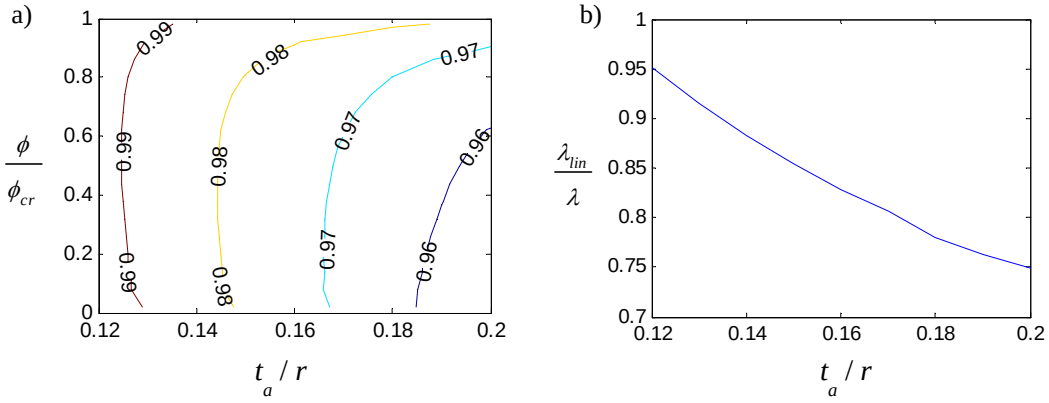

Figure 6: Linearization errors for a semi-circular masonry arch: (a) natural frequency $T_{n,blockeq}$ / $T_{n,wall}$, (b) uplift acceleration λ_{lin} / λ.

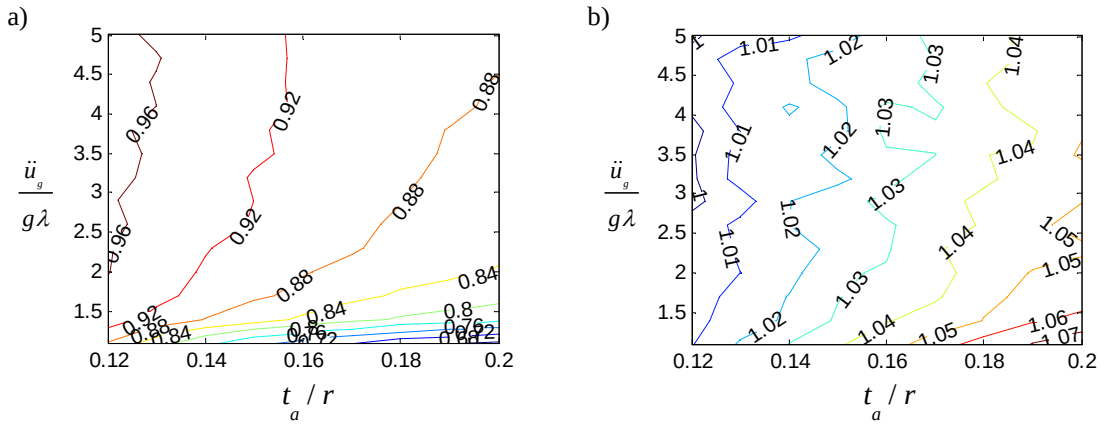

Figure 7: Linearization errors for overturning time ($t_{over,blockeq} / t_{over,wall}$) of a semi-circular masonry arch due to a constant acceleration of amplitude of $\ddot{u}_g / g\lambda$: (a) a_{sc} , (b) $a_{sc,alt}$.

4 EXAMPLE

To exemplify the utility of the equivalence derived in the previous section, the response of an arch (Fig. 8(a)) to the pulse-type Northridge-Rinaldi earthquake record (Fig. 8(b)) will be considered. Rocking response spectra could be produced for the entire earthquake record and used to predict the maximum response of the arch, although this would be computationally intensive. Instead, the primary sinusoidal acceleration pulse within the earthquake (Fig. 8(b)) will be considered alone for prediction purposes.

An approximate closed-form solution [6] for the maximum response of the single rocking block to a single sinusoidal pulse is:

$$\frac{\phi_{max}}{\phi_{cr}} = 1 - \sqrt{1 - \eta^2 \left(1 - D_0^*\right)} \tag{15}$$

where:

$$D_0^* = \left(\frac{\omega}{\omega^2 + 1}\right)^2 \left\{\omega^2 - 2a^2 + 1 + \left(\sqrt{a^2 - 1} + \omega\right) a e^{-\left(2\pi - \sin^{-1}(1/a)\right)/\omega} + \left(\sqrt{a^2 - 1} - \omega\right) a e^{\left(2\pi - \sin^{-1}(1/a)\right)/\omega}\right\} \tag{16}$$

where $a = a_g / (g\lambda)$, $\omega = \omega_g / p$, and a_g and ω_g are the amplitude and circular frequency of the acceleration pulse, respectively. The equivalence derived in §3.2 allows the maximum response of the rocking arch to also be predicted with Eqns. (15) and (16) by using Eqns. (7) and (11) to calculate λ and p.

The predicted maximum response using Eqn. (15) is compared to the full dynamic response predicted using Eqn. (5) in Fig. 8(c,d) for two different geometric scales. In this case, the pulse is dominant, and the maximum response predicted by the two methods is nearly identical. The accuracy of this approach is clearly dependent on whether the pulse dominates the earthquake motion. However, that is true for the single block as well as the arch, and is beside the point of the current paper. Instead, when the pulse does dominate, the results exemplify that the response of a single block can be directly used to predict the response of more complicated structures using the equivalence derived in §3.

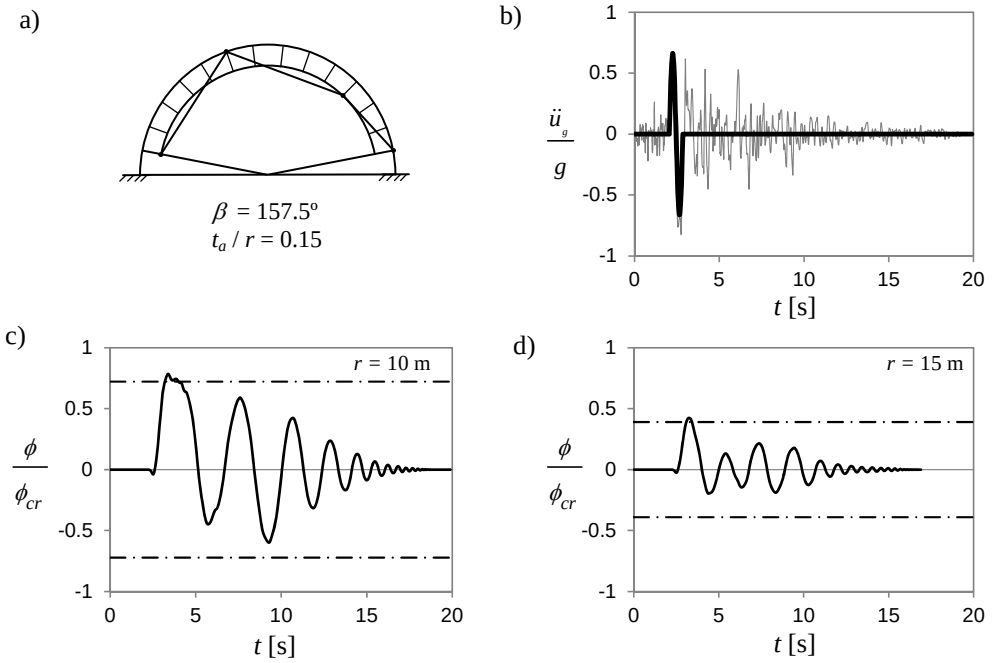

Figure 8: Response of the arch to earthquake motion: (a) arch geoemetry, (b) Northridge-Rinaldi earthquake record with primary impulse highlighted, (c,d) comparison of the arch response calculated using Eqn. (5) (solid line) with the maximum response predicted by Eqn. (15) (dash-dot line) for two different scales (r = 10 m, 15 m).

5 CONCLUSIONS

The objective of this work was to derive an equivalence between the rocking block and a variety of rocking mechanisms in order to develop a unified method for predicting the maximum response of rocking structures during earthquakes. Linearization of the governing equations of motion about the unstable point of equilibrium provided the desired equivalence, although approximate. The error associated with the approximate equivalence was quantified. The results indicate that kinematics complicate the response of the arch, but an alternate scaling relation proved effective in reducing the error caused by linearization. Regardless, the error may be acceptable for seismic assessment where the uncertainty involved in predicting expected ground motions is large.

REFERENCES

[1] G.W. Housner, The behavior of inverted pendulum structures during earthquakes, *Bulletin of the Seismological Society of America*, **53**(2), 403-417, 1963.

[2] P.D. Spanos, A. Koh, Rocking of rigid blocks due to harmonic shaking, *Journal of Engineering Mechanics (ASCE)*, **110**(11), 1627-1642, 1984.

[3] J. Zhang, N. Makris, Rocking response of free-standing blocks under cycloidal pulses, *Journal of Engineering Mechanics (ASCE)*, **127**(5), 473–483, 2001.

[4] M.J. DeJong, Amplification of rocking due to horizontal ground motion, *Earthquake Spectra*, **28**(4), 1405-1421, 2012.

[5] C. Yim, A.K. Chopra, J. Penzien, Rocking response of rigid blocks to earthquakes, *Earthquake Engineering and Structural Dynamics*, **8**(6), 565-587, 1980.

[6] E.G. Dimitrakopoulos, M.J. DeJong, Revisiting the rocking block: Closed form solutions and similarity laws, *Proceedings of the Royal Society A*, **468**(2144), 2294-2318, 2012.

[7] M.J. DeJong, Seismic response of stone masonry spires: Analytical Modeling, *Engineering Structures*, **40**, 556-565, 2012.

[8] M.J. DeJong, C. Vibert, Seismic response of stone masonry spires: Computational and Experimental Modeling, *Engineering Structures*, **40**, 566-574, 2012.

[9] N. Makris, M.F. Vassiliou, Planar rocking response and stability analysis of an array of free-standing columns capped with a freely supported rigid beam, *Earthquake Engineering and Structural Dynamics*, **42**(3), 431–449, 2013.

[10] K. Doherty, M.C. Griffith, N. Lam, J. Wilson, Displacement-based seismic analysis for out-of-plane bending of unreinforced masonry walls, *Earthquake Engineering and Structural Dynamics*, **31**, 833–850, 2002.

[11] D. Ciancio, C. Augarde, Capacity of unreinforced rammed earth walls subject to lateral wind force: elastic analysis versus ultimate strength analysis, *Materials and Structures*, doi: 10.1617/s11527-012-9998-8, 2013.

[12] L. De Lorenzis, M.J. DeJong, J. Ochsendorf, Failure of masonry arches under impulse base motion, *Earthquake Engineering and Structural Dynamics*, **36**, 2119-2136, 2007.

[13] M.J. DeJong, L. De Lorenzis, S. Adams, J.A. Ochsendorf, Rocking stability of masonry arches in seismic regions, *Earthquake Spectra*, **24**(4), 847-865, 2008.

[14] I.J. Oppenheim, The masonry arch as a four-link mechanism under base motion, *Earthquake Engineering and Structural Dynamics*, **21**(11), 1005-1017, 1992.